Searches for Rare Decays at CMS

Kai-Feng Chen[1,*]

[1]Department of Physics, National Taiwan University, Taiwan

Abstract. Rare decays are suppressed in the Standard Model, making them intriguing avenues for exploring new physics beyond the current theoretical framework. Many new physics models could potentially emerge from the study of these decays, providing the insights how the Standard Model could be extended. This proceeding presents the latest studies on rare B meson and τ lepton decays, specifically $B^0_{(s)} \to \mu^+\mu^-$ and $\tau \to 3\mu$, using data collected by the CMS experiment. Additionally, recent observations of $\eta \to 4\mu$ and $J/\psi \to 4\mu$ decays are discussed.

1 Introduction

There are two major methods for probing new physics beyond the Standard Model (SM). The first involves direct searches, looking for heavy new particles produced in high-energy collisions. The second method detects deviations between experimental results and theoretical predictions in rare processes, which have a good chance of revealing new physics contributions indirectly. Both direct and indirect searches are necessary and complement each other in the quest to uncover new physics. This proceeding presents the latest studies on rare $B^0_{(s)} \to \mu^+\mu^-$ decays and $\tau \to 3\mu$ decays, along with observations of $\eta \to 4\mu$ and $J/\psi \to 4\mu$ decays, using data collected by the CMS experiment [1].

These studies heavily rely on the CMS muon system, which consists of three different devices: drift tubes, cathode strip chambers, and resistive plate chambers, providing extensive coverage up to $|\eta| < 2.4$. The typical resolution of the dimuon invariant mass ranges from 0.6% to 1.5%, depending on the rapidity. The muon system also offers excellent muon identification capabilities, with a fake rate of below 0.1% for charged kaons and pions, and even lower for protons. For some analyses, such as the $B^0_{(s)} \to \mu^+\mu^-$ studies, dedicated multivariate analysis-based identification method is introduced to further suppress fake candidates. The CMS trigger system is composed of a fast hardware trigger and a software-based high-level trigger with full tracking and vertex reconstruction. Many CMS flavor physics analyses rely on quarkonia triggers, such as $J/\psi \to \mu^+\mu^-$ and $\Upsilon \to \mu^+\mu^-$, including displaced or non-displaced conditions, as well as non-resonant dimuon and three-muon triggers. There is also a dedicated $B^0_{(s)} \to \mu^+\mu^-$ trigger to preserve potential signal events. As luminosity increases, trigger requirements are tightened, but special data streams, known as “scouting" and “parking," are used to extend the actual capabilities.

*e-mail: Kai-Feng.Chen@cern.ch

2 Measurement of $B_s^0 \to \mu^+\mu^-$ and Search for $B^0 \to \mu^+\mu^-$

The $B^0_{(s)} \to \mu^+\mu^-$ decays can only proceed through flavor-changing neutral current processes and are highly suppressed in the SM. These processes are theoretically robust in their predictions [2–4] and have a high potential to be influenced by unknown particles, making them an excellent place to search for new physics. The typical observables include the decay branching fractions and the effective lifetime of $B_s^0 \to \mu^+\mu^-$ events. The decay branching fraction of $B_s^0 \to \mu^+\mu^-$ has been well measured by the ATLAS, CMS, and LHCb experiments [5–7], while more data is needed to find the first evidence of $B^0 \to \mu^+\mu^-$. In the SM, only the heavy B_s^0 state, which has a slightly longer lifetime, can decay into dimuons. The introduction of new physics could allow for a different composition of states. Thus, the effective lifetime of $B_s^0 \to \mu^+\mu^-$ is also an essential observable, defined as follows:

$$\tau_{\mu^+\mu^-} = \frac{\int_0^\infty t\Gamma(B_s^0(t) \to \mu^+\mu^-)\,dt}{\int_0^\infty \Gamma(B_s^0(t) \to \mu^+\mu^-)\,dt} = \frac{\tau_{B_s^0}}{1-y_s^2}\left(\frac{1 + 2\mathcal{A}_{\Delta\Gamma}^{\mu^+\mu^-} y_s + y_s^2}{1 + \mathcal{A}_{\Delta\Gamma}^{\mu^+\mu^-} y_s}\right), \tag{1}$$

where $\mathcal{A}_{\Delta\Gamma}^{\mu^+\mu^-} = -\mathcal{R}(\lambda)/(1+|\lambda|^2)$ and $y_s = \tau_{B_s^0}\Delta\Gamma_s/2$.

The signal signature of $B^0_{(s)} \to \mu^+\mu^-$ consists of two muons originating from a single displaced vertex, isolated from other activities. The momentum of the $B^0_{(s)} \to \mu^+\mu^-$ candidate should align with its flight direction. The major background sources are combinatorial events, primarily involving muons from semileptonic b-hadron decays or misidentified charged hadrons. Rare background processes include doubly-misidentified hadrons from two-body decays such as $B \to K^+\pi^-$, $\pi^+\pi^-$, and K^+K^-, which form a broad peak structure near the signal. Additionally, non-peaking three-body decays like $B \to h^-\mu^+\nu$ and $B \to h\mu^+\mu^-$, where h denotes a kaon or pion, contribute to the background in a lower mass region.

Given the small signal compared to the combinatorial background, powerful background suppression is essential. This is achieved by selecting high-quality muons, ensuring a well-reconstructed secondary vertex, precise dimuon mass resolution, and other kinematic information. Muon candidates are selected using a strict identification requirement based on a boosted decision tree (BDT) classifier, optimized with tracking and muon-related detector information, achieving a fake rate below 0.1%.

The branching fractions are normalized using $B^+ \to J/\psi K^+$ or $B_s^0 \to J/\psi\phi$ decays, allowing for the first-order cancellation of systematic uncertainties. The master formulas for the branching fractions are:

$$\mathcal{B}(B_s^0 \to \mu^+\mu^-) = \mathcal{B}(B^+ \to J/\psi K^+)\frac{N_{B_s^0\to\mu^+\mu^-}}{N_{B^+\to J/\psi K^+}}\frac{\epsilon_{B^+\to J/\psi K^+}}{\epsilon_{B_s^0\to\mu^+\mu^-}}\frac{f_u}{f_s}, \tag{2}$$

$$\mathcal{B}(B_s^0 \to \mu^+\mu^-) = \mathcal{B}(B_s^0 \to J/\psi\phi)\frac{N_{B_s^0\to\mu^+\mu^-}}{N_{B_s^0\to J/\psi\phi}}\frac{\epsilon_{B^+\to J/\psi\phi}}{\epsilon_{B_s^0\to\mu^+\mu^-}}, \tag{3}$$

$$\mathcal{B}(B^0 \to \mu^+\mu^-) = \mathcal{B}(B^+ \to J/\psi K^+)\frac{N_{B^0\to\mu^+\mu^-}}{N_{B^+\to J/\psi K^+}}\frac{\epsilon_{B^+\to J/\psi K^+}}{\epsilon_{B^0\to\mu^+\mu^-}}, \tag{4}$$

where the yields and selection efficiencies for each process are given by N_X and ϵ_X (where $X = B_s^0 \to \mu^+\mu^-$, $B^0 \to \mu^+\mu^-$, $B^+ \to J/\psi K^+$, or $B_s^0 \to J/\psi\phi$). The fragmentation ratio $f_s/f_u = 0.231 \pm 0.008$, along with the branching fractions of the normalization channels $\mathcal{B}(B^+ \to J/\psi K^+)$ and $\mathcal{B}(B_s^0 \to J/\psi\phi)$, are treated as external inputs. The value of f_s/f_u is derived from p_T-dependent measurements from LHCb [8], integrated over the effective p_T distribution from the CMS analysis. This ratio has been verified using $B^+ \to J/\psi K^+$ and $B_s^0 \to J/\psi\phi$ data. Rare background processes are normalized using a similar setup.

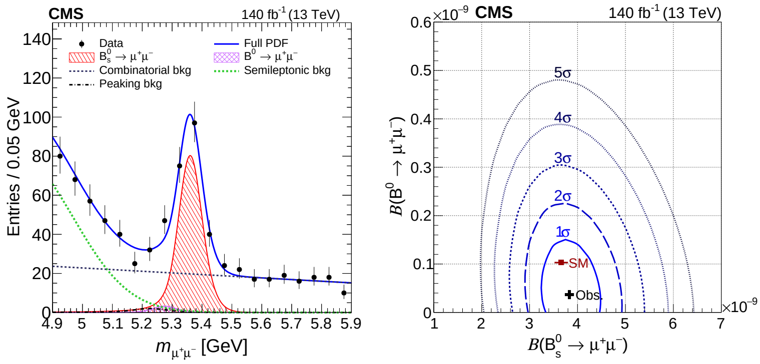

Figure 1. The dimuon invariant mass distribution (left) for the candidates with $d_{\text{MVA}} > 0.99$. The solid blue curves represent the projections of fit model. The profile likelihood (right) in $\mathcal{B}(B^0 \to \mu^+\mu^-)$ versus $\mathcal{B}(B_s^0 \to \mu^+\mu^-)$ plane, while the contours enclose the regions with 1σ-5σ coverage. Figures are from Ref. [6].

An improved event classification BDT (denoted as d_{MVA}), trained using topological and kinematic variables with the XGBoost package, provides excellent discrimination power between signal and combinatorial background events. The performance of d_{MVA} is calibrated using $B^+ \to J/\psi K^+$ events. To match the kinematics between $B^+ \to J/\psi K^+$ and $B_s^0 \to \mu^+\mu^-$ decays, additional requirements are introduced in this calibration study, such as ensuring the kaon from the B^+ decay has a soft $p_T < 1.5$ GeV and scaling the flight-length significance by a factor of 1.6. A dedicated XGBoost classifier is trained to align the resulting distributions from simulation with those from data. The performance of d_{MVA} demonstrates approximately twice the signal efficiency for the same background level compared to the previous iteration of the analysis, with manageable systematic uncertainties of 2%-3%.

The branching fractions of $B_{(s)}^0 \to \mu^+\mu^-$ decays are extracted using an extended unbinned maximum likelihood estimator, yielding:

$$\mathcal{B}(B_s^0 \to \mu^+\mu^-) = \left[3.83^{+0.38}_{-0.36}\,(\text{stat})^{+0.19}_{-0.16}\,(\text{syst})^{+0.14}_{-0.13}\,(f_s/f_u)\right] \times 10^{-9}, \tag{5}$$

$$\mathcal{B}(B^0 \to \mu^+\mu^-) = \left[0.37^{+0.75}_{-0.67}\,(\text{stat})^{+0.08}_{-0.09}\,(\text{syst})\right] \times 10^{-10}. \tag{6}$$

Alternatively, the $B_s^0 \to \mu^+\mu^-$ branching fraction is obtained with $B_s^0 \to J/\psi\phi$ as the normalization, leading to:

$$\mathcal{B}(B_s^0 \to \mu^+\mu^-) = \left[4.02^{+0.40}_{-0.38}\,(\text{stat})^{+0.28}_{-0.23}\,(\text{syst})^{+0.18}_{-0.15}\,(\mathcal{B})\right] \times 10^{-9}, \tag{7}$$

where the last uncertainty arises from the $B_s^0 \to J/\psi\phi$ branching fraction uncertainty. The upper limit on the decay branching fraction of $B^0 \to \mu^+\mu^-$ is derived as:

$$\mathcal{B}(B^0 \to \mu^+\mu^-) < 1.9 \times 10^{-10}, \tag{8}$$

using the full CL_s prescription at 95% confidence level. Figure 1 shows the dimuon invariant mass distribution from the categories with higher signal purities. The profile likelihood contours enclosing regions with coverages of 1-5 standard deviations are also presented. The effective lifetime of $B_s^0 \to \mu^+\mu^-$ events is extracted with a three-dimensional maximum likelihood fit to the invariant mass, decay time, and decay time uncertainty distributions, yielding:

$$\tau_{\mu^+\mu^-} = 1.83^{+0.23}_{-0.20}\,(\text{stat})^{+0.04}_{-0.04}\,(\text{syst})\ \text{ps}, \tag{9}$$

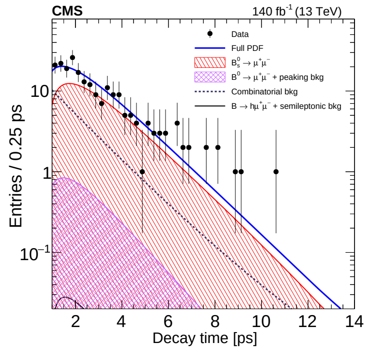

Figure 2. The proper decay time distribution for the $B_s^0 \to \mu^+\mu^-$ candidates, with the result of the fit superimposed. Figure is from Ref. [6].

which is consistent with the SM prediction. The decay time distribution for the candidate events in the dimuon invariant mass region ranging from 5.28 GeV to 5.48 GeV is shown in Fig. 2. These results, including the decay branching fraction and effective lifetime of $B_s^0 \to \mu^+\mu^-$, represent the best single measurements to date.

3 Search for $\tau^- \to \mu^-\mu^+\mu^-$ Decay

The decay of a τ lepton into three muons without any missing neutrinos is a charged lepton flavor-violating process. In the SM, such a decay is only permitted through neutrino oscillations, resulting in an extraordinarily small branching fraction on the order of 10^{-53} to 10^{-56}, which is far beyond experimental accessibility. However, the decay rate can be significantly enhanced under new physics scenarios. For instance, introducing right-handed Dirac neutrinos can increase the decay rate to the order of 10^{-18}. Some supersymmetric scenarios could further raise the branching fraction to the order of 10^{-7} to 10^{-10}, aligning with the target sensitivities of modern collider experiments. Moreover, a three-muon final state is highly accessible and experimentally clean, making the search for this decay an excellent probe for physics beyond the SM. The best limit on the decay branching fraction to date, $\mathcal{B}(\tau^- \to \mu^-\mu^+\mu^-) < 1.9 \times 10^{-8}$ at 90% confidence level, was given by the Belle-II experiment [9].

In the recent CMS analysis [10], two major sources of τ leptons were considered: those originating from heavy flavor mesons and those from W boson decays. The τ leptons from heavy flavor mesons are the dominant source, yielding approximately 10^{11} τ's per fb^{-1} of data. However, these τ leptons typically have lower p_T and larger $|\eta|$, resulting in lower trigger efficiency. Additionally, this analysis is more prone to selecting fake muon candidates decaying from hadrons. On the other hand, although τ leptons from W boson decays occur at a much lower rate, around 10^7 τ's per fb^{-1} of data, they generally possess higher p_T and are more centrally within the detector, leading to higher trigger efficiency. Furthermore, the kinematic features associated with W boson decays, such as significant missing transverse energy and relatively lower hadronic activity, provide additional handles for background suppression.

The analysis starts from the events selected with dedicated designed high-level triggers, such as three isolated muons for W-boson channel, and two muons with one additional track, or simple three muons for the heavy flavor channel. The signal candidate is reconstructed with

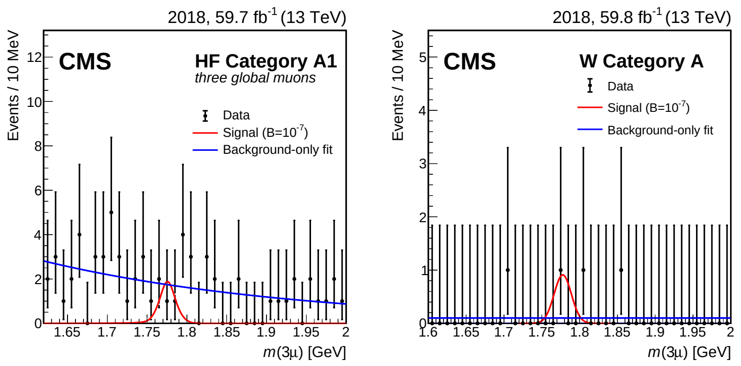

Figure 3. Three-muon invariant mass distributions, for the events in the highest BDT score and best mass resolution category, for the heavy flavor (left) and W-boson (right) channels, from the data collect in 2018. Figures are from Ref. [10].

three muons at offline analysis, with sum of their changes to be ± 1. The dominant background is combinatorial events, which are mostly consistent with two real muons, plus a fake muon candidate from hadrons decays, for example, a cascade $B \to D + \mu + X$, $D \to \mu + \nu + K$, $K \to \mu$ decay. In order to suppress fake muon from low momentum hadron, a dedicated BDT classifier is trained using simulated signal events and fake muon candidates from hadrons. Those background sources with three genuine muons, while two of them originated from ϕ or ω resonances, are actively rejected according to their invariant masses. The background from electroweak process, such as $W \to \mu\nu$ with additional final state radiations, is removing by requiring on the displacement from the interaction point.

A BDT-based event classifier has been introduced to further suppress background events. The classifier is trained using simulated $\tau^- \to \mu^-\mu^+\mu^-$ signals and data sideband events as proxies for background processes. Key features used as inputs include kinematic information (such as momentum and missing energy), topological information (quality of vertex finding, pointing angle, and isolation variables), and other relevant data (such as muon identification BDT scores). Separate BDTs are constructed for different channels, and scale factors are applied to the simulated samples to account for potential discrepancies between data and simulations.

To maximize statistical power, events are categorized based on the three-muon invariant mass resolution, creating three categories (low, medium, and best resolutions) for each data-taking year and production channel. The signal $\tau^- \to \mu^-\mu^+\mu^-$ decay is then extracted using a simultaneous extended unbinned maximum likelihood fit to the three-muon invariant mass distributions. The invariant mass distributions for the 2018 dataset, covering both heavy flavor and W-boson channels, are shown in Fig. 3. From the fit, no signal was observed, hence an upper limit on the $\tau^- \to \mu^-\mu^+\mu^-$ decay branching fraction is set. After combining the results with the previous publication [11] using the data collected in 2016, the upper limits are:

$$\mathcal{B}(\tau^- \to \mu^-\mu^+\mu^-) < 3.6 \times 10^{-8} \text{ (95\% confidence level)}, \tag{10}$$

$$< 2.9 \times 10^{-8} \text{ (90\% confidence level)}, \tag{11}$$

as shown in Fig. 4. This result is only 50% higher than the best limit set by Belle-II and have the potential for further improvement with upcoming CMS data.

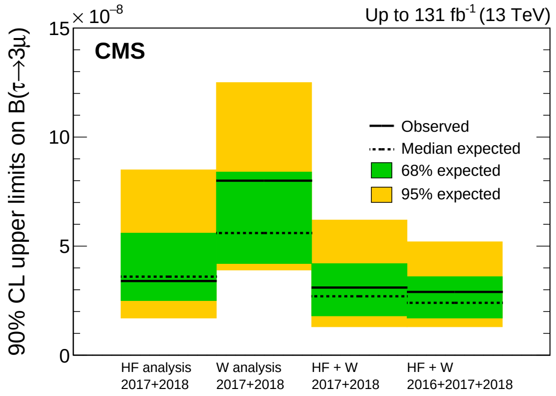

Figure 4. Observed and expected upper limits on $\mathcal{B}(\tau^- \to \mu^-\mu^+\mu^-)$ decay at at the 90% confidence level, for the heavy flavor channel, the W-boson channel, and the combination of the two, as well as the combination with the result based on 2016 data. Figure is from Ref. [10].

4 Observation of $\eta \to 4\mu$ and $J/\psi \to 4\mu$ Decays

In the SM, the decay $\eta \to 4\mu$ is predicted to have a very low branching fraction of $O(10^{-9})$. However, this process is sensitive to new physics scenarios and serves as a precision test of the SM. At the CMS experiment, this analysis is feasible using the "data scouting" technique, which reduces event size to accelerate data acquisition and circumvent computing power and bandwidth limitations of regular trigger thresholds. Information at the high-level triggers is stored, bypassing standard prompt event processing steps. This allows for the exploration of rare decays in very low momentum regions due to relaxed muon thresholds.

By analyzing 101 fb^{-1} of CMS scouting data, a clear peak for the $\eta \to 4\mu$ signal has been observed [12], as shown in Fig. 5. A fit to the four-muon invariant mass distribution revealed around 50 signal events with a statistical significance greater than five standard deviations. The total number of produced η mesons was estimated using the normalization channel $\eta \to 2\mu$. Corrections for efficiency and acceptance differences between the $\eta \to 4\mu$ and $\eta \to 2\mu$ decays were calculated using simulated samples. The resulting branching fraction is:

$$\mathcal{B}(\eta \to \mu^+\mu^-\mu^+\mu^-) = \left[5.0 \pm 0.8\,(\text{stat}) \pm 0.7\,(\text{syst}) \pm 0.7\,(\mathcal{B}_{\eta\to\mu^+\mu^-})\right] \times 10^{-9}. \tag{12}$$

This result is consistent with the SM prediction of $3.98 \pm 0.15 \times 10^{-9}$. Further studies showed a good description of the four-muon kinematic spectrum for the events near the signal peak.

Thanks to the large production rate provided by the LHC and the excellent performance of the CMS muon system, the exploration of very rare decays involving multiple muons, such as $J/\psi \to 4\mu$, becomes feasible. Other lepton flavor combinations, such as $J/\psi \to 4e$ and $J/\psi \to 2e2\mu$, have already been observed by the BES-III experiment. These rare decays serve as novel testing grounds for quantum electrodynamics predictions within the SM. At the CMS experiment, this study utilizes the "B-Parking" scenario, which employs a specialized trigger requiring only one muon at the trigger level and a dedicated data storage strategy. This strategy bypasses prompt reconstruction procedures, instead "parking" the data for further analysis. This scenario was implemented during the 2018 data-taking period, resulting in a b-hadron enriched dataset.

By reconstructing the four-muon final state, a narrow peak at the known J/ψ mass was found in the CMS analysis [13]. A maximum likelihood fit to the invariant mass distribution

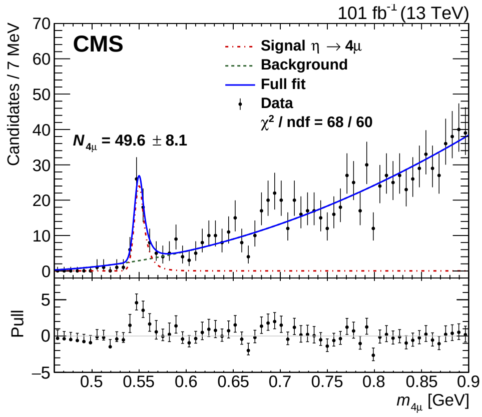

Figure 5. The measured invariant mass distribution of four muons near the η meson, with the result of the fit overlaid. Figure is from Ref. [12].

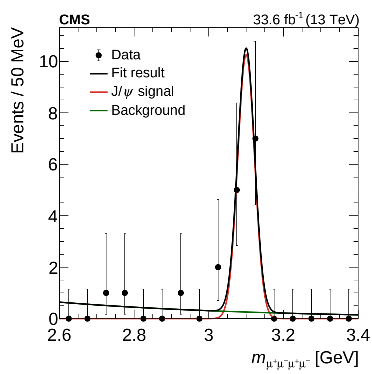

Figure 6. Measured four-muon mass distributions for the $J/\psi \to 4\mu$ candidates. The solid black line shows the result of the fit. Figure is from Ref. [13].

yielded around 12 signal candidates, as shown in Fig. 6. Normalizing this finding with respect to the large number of $J/\psi \to 2\mu$ events, the resulting decay branching fraction is:

$$\mathcal{B}(J/\psi \to \mu^+\mu^-\mu^+\mu^-) = \left[10.1^{+3.3}_{-2.7}\,(\text{stat}) \pm 0.4\,(\text{syst})\right] \times 10^{-7}. \tag{13}$$

This result is consistent with the SM prediction of $9.74 \pm 0.05 \times 10^{-7}$. This rare decay has also been observed by the LHCb experiment [14].

5 Summary

Thanks to the excellent muon performance and dynamic trigger configurations, the CMS experiment plays a key role in flavor physics, particularly in the search for rare decays. The latest studies of $B^0_{(s)} \to \mu^+\mu^-$ decays show results consistent with the Standard Model predictions, potentially bringing the average $B^0_s \to \mu^+\mu^-$ branching fraction even closer to the predicted value. By examining both heavy flavor and W-boson decays, CMS has updated the upper limit on the rare $\tau \to 3\mu$ decay branching fraction using the full Run-2 data. This new limit approaches the best result to date from the B-factory. Furthermore, the implementation of the scouting and parking scenarios by the CMS experiment has extended the capabilities of the trigger system, allowing for studies at the lowest possible thresholds. This has led to the observation of very rare decays such as $\eta \to 4\mu$ and $J/\psi \to 4\mu$. With the upcoming dataset collected during LHC Run-3, CMS is expected to explore regions beyond the current scope, potentially uncovering new physics phenomena.

References

[1] S. Chatrchyan *et al.* [CMS], "The CMS Experiment at the CERN LHC," JINST **3**, S08004 (2008) doi:10.1088/1748-0221/3/08/S08004.

[2] M. Beneke, C. Bobeth and R. Szafron, "Power-enhanced leading-logarithmic QED corrections to $B_q \to \mu^+\mu^-$," JHEP **10**, 232 (2019) [erratum: JHEP **11**, 099 (2022)] doi:10.1007/JHEP10(2019)232 [arXiv:1908.07011 [hep-ph]].

[3] M. Beneke, C. Bobeth and R. Szafron, "Enhanced electromagnetic correction to the rare *B*-meson decay $B_{s,d} \to \mu^+\mu^-$," Phys. Rev. Lett. **120**, no.1, 011801 (2018) doi:10.1103/PhysRevLett.120.011801 [arXiv:1708.09152 [hep-ph]].

[4] C. Bobeth, M. Gorbahn, T. Hermann, M. Misiak, E. Stamou and M. Steinhauser, "$B_{s,d} \to l^+l^-$ in the Standard Model with Reduced Theoretical Uncertainty," Phys. Rev. Lett. **112**, 101801 (2014) doi:10.1103/PhysRevLett.112.101801 [arXiv:1311.0903 [hep-ph]].

[5] M. Aaboud *et al.* [ATLAS], "Study of the rare decays of B^0_s and B^0 mesons into muon pairs using data collected during 2015 and 2016 with the ATLAS detector," JHEP **04**, 098 (2019) doi:10.1007/JHEP04(2019)098 [arXiv:1812.03017 [hep-ex]].

[6] A. Tumasyan *et al.* [CMS], "Measurement of the $\mathrm{B}^0_\mathrm{S}\to\mu^+\mu^-$ decay properties and search for the $\mathrm{B}^0\to\mu^+\mu^-$ decay in proton-proton collisions at $\sqrt{s}$ = 13 TeV," Phys. Lett. B **842**, 137955 (2023) doi:10.1016/j.physletb.2023.137955 [arXiv:2212.10311 [hep-ex]].

[7] R. Aaij *et al.* [LHCb], "Analysis of Neutral B-Meson Decays into Two Muons," Phys. Rev. Lett. **128**, no.4, 041801 (2022) doi:10.1103/PhysRevLett.128.041801 [arXiv:2108.09284 [hep-ex]].

[8] R. Aaij *et al.* [LHCb], "Precise measurement of the f_s/f_d ratio of fragmentation fractions and of B^0_s decay branching fractions," Phys. Rev. D **104**, no.3, 032005 (2021) doi:10.1103/PhysRevD.104.032005 [arXiv:2103.06810 [hep-ex]].

[9] I. Adachi *et al.* [Belle-II], "Search for lepton-flavor-violating $\tau^- \to \mu^-\mu^+\mu^-$ decays at Belle II," [arXiv:2405.07386 [hep-ex]].

[10] A. Hayrapetyan *et al.* [CMS], "Search for the lepton flavor violating $\tau \to 3\mu$ decay in proton-proton collisions at $\sqrt{s}$ = 13 TeV," Phys. Lett. B **853**, 138633 (2024) doi:10.1016/j.physletb.2024.138633 [arXiv:2312.02371 [hep-ex]].

[11] A. M. Sirunyan *et al.* [CMS], "Search for the lepton flavor violating decay $\tau \to 3\mu$ in proton-proton collisions at $\sqrt{s}$ = 13 TeV," JHEP **01**, 163 (2021) doi:10.1007/JHEP01(2021)163 [arXiv:2007.05658 [hep-ex]].

[12] A. Hayrapetyan *et al.* [CMS], "Observation of the rare decay of the η meson to four muons," Phys. Rev. Lett. **131**, no.9, 091903 (2023) doi:10.1103/PhysRevLett.131.091903 [arXiv:2305.04904 [hep-ex]].

[13] A. Hayrapetyan *et al.* [CMS], "Observation of the J/$\psi\to\mu$+μ-μ+μ- decay in proton-proton collisions at s=13 TeV," Phys. Rev. D **109**, no.11, L111101 (2024) doi:10.1103/PhysRevD.109.L111101 [arXiv:2403.11352 [hep-ex]].

[14] LHCb Collaboration, "Observation of the J/$\psi\to\mu$+μ-μ+μ- decay in proton-proton collisions at s=13 TeV," LHCb-CONF-2024-001 [https://cds.cern.ch/record/2894330].